AGU ADVANCING EARTH AND SPACE SCIENCES

JGR Solid Earth

RESEARCH ARTICLE
10.1029/2023JB027192

Shear-Wave Splitting Reveals Layered-Anisotropy Beneath the European Alps in Response to Mediterranean Subduction

F. Link[1,2] and G. Rümpker[1,3]

[1]Institute of Geosciences, Goethe-University Frankfurt, Frankfurt, Germany, [2]Department of Planetary Sciences, Yale University, New Haven, CT, USA, [3]Frankfurt Institute for Advanced Studies, Frankfurt, Germany

Key Points:

- This study presents the first comprehensive analysis of layered anisotropy for the entire Alpine range based on shear-wave splitting
- The anisotropy patterns within the asthenosphere and lithosphere suggest a relation to large-scale Mediterranean tectonic processes
- Our findings allow discrimination between subduction-controlled asthenospheric flow and tectonic deformation of the lithosphere

Supporting Information:

Supporting Information may be found in the online version of this article.

Correspondence to:

F. Link,
frederik.link@yale.edu

Citation:

Link, F., & Rümpker, G. (2023). Shear-wave splitting reveals layered-anisotropy beneath the European Alps in response to Mediterranean subduction. *Journal of Geophysical Research: Solid Earth, 128*, e2023JB027192. https://doi.org/10.1029/2023JB027192

Received 31 MAY 2023
Accepted 2 SEP 2023

Author Contributions:

Conceptualization: F. Link, G. Rümpker
Formal analysis: F. Link
Funding acquisition: G. Rümpker
Investigation: F. Link
Methodology: F. Link, G. Rümpker
Project Administration: G. Rümpker
Supervision: G. Rümpker
Visualization: F. Link
Writing – original draft: F. Link
Writing – review & editing: F. Link, G. Rümpker

Abstract The European Alps formed at the boundary between the Eurasian plate and Adriatic microplate within a complex system of collision and subduction. However, the large-scale three-dimensional mantle-flow field related to the underlying geodynamic processes has not yet been resolved in detail. In this study, we present the first comprehensive analysis of layered anisotropy for the complete Alpine range from shear-wave splitting measurements at 591 seismic stations of the AlpArray experiment. Our findings suggest a combination of asthenospheric and distinct lithospheric contributions to the splitting observations, which can be seen as a generalization of previously reported models of single-layer anisotropy. The enhanced vertical resolution exposes the impact of successive Mediterranean tectonic episodes, such as the opening of the Provençal-Ligurian and Tyrrhenian Basins alongside the Adriatic slab retreat, as well as the Pannonian Basin opening and the Aegean slab retreat, resulting in deformation of the lithosphere and flow in the asthenospheric mantle. The dominant role of the larger scale Mediterranean subduction systems on mantle dynamics becomes evident. The observations provide supporting evidence that the Eurasian slab has broken off at its boundaries and that the resulting gaps channel flow from the mantle beneath the Eurasian plate to the Adriatic and Aegean subduction systems. The results provide new constraints on geodynamic processes involved in forming the European Alps, as previous tectonic episodes are preserved in the anisotropic fabric of the lithosphere-asthenosphere system. This raises new questions regarding their geochemical and geophysical conditions, and their larger-scale impact on the formation of the Alpine orogeny.

Plain Language Summary The European Alps are located along the contact of the Eurasian continental plate to the North and the Adriatic plate to the South. This zone is subject of a complicated history of their collision, in which the rigid plates are consumed into the more flexible and softer underlying mantle. In this work, we look at seismic anisotropy which describes the property of rocks to allow body waves to travel with different speeds when passing through the rock at different directions. This is mostly produced by a flow of softer rock beneath the rigid outer shell of the Earth. In our analysis of anisotropy, we also allow for its change with depth. We find that the anisotropy is not only produced by flow, but in part also by separate volumes of the rigid outer shell. This is a result from a history of deformation. While the location of the Eurasian and Adriatic plates remains unchanged, heavy parts of the plates descent. As a result, the plates are stretched forming the thinned Liguro-Provençal and Pannonian Basin. In addition, the descending Eurasian plate is breaking off at its boundaries, which allows the softer rock at larger depth to flow through the resulting gaps.

1. Introduction

The European Alps were formed as a result of the collision between the Eurasian and African plates, which began at about 35 Ma with the Adriatic microplate indenting into the former (Dewey et al., 1973, 1989; Handy et al., 2010, see Figure 1). The uplift of the Alps occurred following the southward subduction of oceanic lithosphere beneath the Adriatic plate (Handy et al., 2010; Schmid et al., 2004). Concurrently, the Adriatic plate plunged eastward beneath the Eurasian plate, giving rise to the Dinarides (Handy et al., 2010, 2015; Kissling et al., 2006; Lippitsch, 2003; Schmid et al., 2008; Ustaszewski et al., 2008). The subduction and retreat of the Adriatic microplate at its western edge led to the formation of the Apennines and caused stretching of the Eurasian plate beneath the Ligurian and Tyrrhenian Seas, resulting in the formation of back-arc basins (Faccenna et al., 2004; Handy et al., 2015; Laubscher, 1988; Malinverno & Ryan, 1986; Moretti & Royden, 1988; Royden, 1993; Vignaroli et al., 2008). These tectonic sequences were accompanied by breakoff events, which may have been a consequence of the continental collision between the Eurasian and African plates that occurred as the Tethyan oceanic unit was entirely consumed (Kästle et al., 2020).

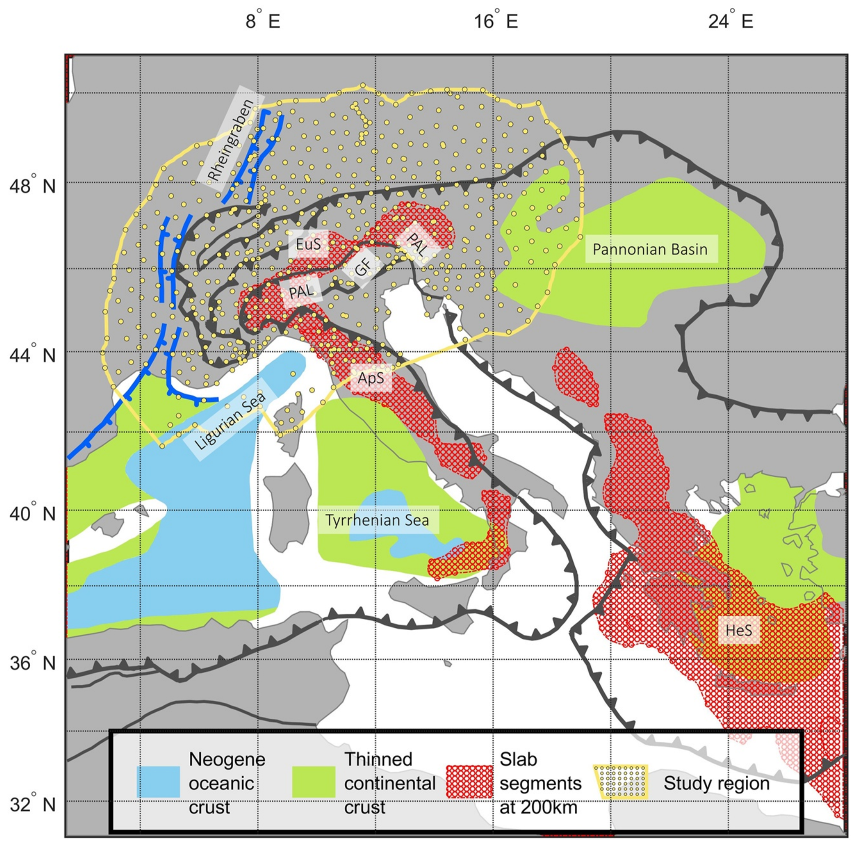

Figure 1. Simplified tectonic map highlighting extensional basins in the Mediterranean area (Platt, 2007) and slab anomalies at 200 km, which we compiled from recent tomographic studies (Kästle et al., 2018, 2020; Koulakov et al., 2009; Paffrath et al., 2021; Zhao et al., 2016). Important geologic features for this study are labeled with abbreviations EuS—Eurasian Slab, PAL—Periadriatic Line, GF—Giudicarie Fault, ApS—Adriatic Slab and HeS—Aegean Slab. The stations of the AlpArray network (AlpArray Seismic Network, 2015; Hetényi et al., 2018) and permanent stations used in this study are indicated by yellow dots and evenly cover the greater Alpine region marked by a yellow contour.

Such a complex tectonic history would have a considerable impact on the underlying lithosphere–asthenosphere interactions and the mantle flow field (Faccenna et al., 2014; Long & Becker, 2010). Mantle deformation can cause seismically anisotropic minerals, such as olivine, to align along the main flow direction (Karato et al., 2008; Silver, 1996). This large-scale seismic anisotropy causes splitting of a seismic shear wave when it enters an anisotropic medium. The resulting two phases are orthogonally polarized in the fast (ϕ; measured here clockwise relative to north) and slow directions, and the velocity difference between these phases in the anisotropic layer causes a time delay (also called the delay time, δt) that increases with the extension and strength of anisotropy within the medium. Analysis of shear-wave splitting of converted (XKS) phases from the core-mantle boundary is a widely used method for robustly inferring the orientation and magnitude of seismic anisotropy and, thus, the mantle flow field (Savage, 1999; Silver & Chan, 1991). Present-day flow is responsible for anisotropy in the asthenosphere, while the fabrics and lineations frozen in the lithosphere due to previous tectonic events can also produce anisotropic material properties (Long & Becker, 2010; Savage, 1999). Furthermore, the lithosphere responds to tectonic strains, which can produce coherent anisotropy across the crust and uppermost mantle (Silver, 1996).

Numerous shear-wave splitting studies have been conducted in the greater Alpine region, suggesting an apparently simple anisotropic pattern which seems to contradict its complex tectonic history. The orogen-parallel fast directions beneath the Central and Western Alps, as well as the anisotropy in SE France and the Ligurian Sea have been traditionally associated with a dominant "toroidal" (orogen parallel) asthenospheric flow field where the flow is more-or-less perpendicular to the direction of compression and exhibits only minor depth variations (Barruol et al., 2004; Hein et al., 2021; Lucente et al., 2006; Margheriti et al., 1996; Salimbeni et al., 2008). The studies suggest that this characteristic flow pattern results from the northward retreat of the Eurasian slab and the

10.1029/2023JB027192

suction caused by the retreating Apenninic subduction. These processes are possibly accompanied by lithospheric anisotropy produced by the compressional regime of the Alpine orogeny (Vinnik et al., 1994). Another consistent feature in these studies is the clockwise rotation of ~40° in the fast-axis orientation from the Western and Central Alps to the Eastern Alps (Bokelmann et al., 2013; Hein et al., 2021; Plenefisch et al., 2001; Qorbani et al., 2015), suggesting different mantle deformation mechanisms beneath these two regions.

Some previous studies have also reported layered anisotropy in isolated regions of the Alpine arc (Plenefisch et al., 2001; Qorbani et al., 2015; Salimbeni et al., 2008; Vinnik et al., 1994; Walther et al., 2014). The corresponding orientations and magnitudes were quantified by fitting the characteristic azimuthal variations (Silver & Savage, 1994) in the measured splitting parameters (ϕ, δt) at individual seismic stations or were derived from the analysis of characteristics found at station clusters within a localized dense network (Link & Rümpker, 2021). However, no systematic shear-wave splitting analysis has been conducted to identify multiple layers of anisotropy and three-dimensional mantle flow for the greater Alpine region. The tectonic implications of such study could help to reconcile the complex surface structure with the measured anisotropy. To perform a detailed analysis of the splitting characteristics in the greater Alpine region with high lateral resolution, we utilize the recently established AlpArray network (AlpArray Seismic Network, 2015; Hetényi et al., 2018) (see Figure 1). The unprecedented data coverage, in combination with improved constraints on anisotropic layering obtained through joint shear-wave splitting analysis of all measured events at individual stations (Link et al., 2022), provides new detailed insights into possible lithosphere–asthenosphere interactions in the vicinity of the European Alps.

2. Methods and Data Analyses

2.1. Data Processing and Single Event Splitting Analysis

We analyzed core-mantle converted phases, for example, SKS, SKKS, SKIKS, PKS, PKKS, and PKIKS, for shear-wave splitting, that were recorded at 591 permanent (network codes BW, CH, CR, CZ, FR, GE, GR, GU, HU, IU, IV, MN, NI, OE, OX, RD, RF, SI, SK, SL, ST), ocean bottom seismometers (OBS) and temporary stations (network code Z3) in the AlpArray network (AlpArray Seismic Network, 2015; Hetényi et al., 2018) using the automated SplitRacer toolbox (Link et al., 2022). A detailed list of all stations contributing to this study is provided in the supplements. All data is accessible via the ORFEUS or IRIS data centers. We selected earthquakes recorded by each station from their initial deployment until the end of September 2020, providing recording periods ranging from 35 years for some permanent stations to only 9 months for stations of the ocean bottom experiment. We chose earthquakes above a magnitude threshold of 5.8 and with epicentral distances between 89° and 140°. The data were bandpass-filtered using a second order Butterworth filter with corner periods of 4 and 50 s. Preliminary windows of 100 s are centered around theoretical arrival times for core-mantle converted phases based on the 1D velocity model iasp91 (Kennett & Engdahl, 1991). In a first quality check, to retain as much analyzable data as possible while minimizing the computation time, events were discarded if they had a signal-to-noise ratio of less than 2.5 for permanent stations, 1.8 for temporary stations and 1.2 for OBS stations. The remaining phases were automatically cut from the preliminarily selected windows based on a time-frequency analysis (Link et al., 2022). As part of this process, only high-quality phases are kept for analysis as the automatic algorithm requires significant signal amplitude levels to identify a dominant wavelet. This is tested against an STA/LTA criterion. The resulting phases are analyzed for their long period polarization (between 15 and 50 s). This allows to identify and measure station misorientations (see Table S1) as the long-period particle motion is confined to the great-circle plane connecting source and receiver (see also Rümpker & Silver, 1998). The splitting analysis in the SplitRacer toolbox is based on the transverse energy minimization technique (Silver & Chan, 1991) to derive the delay time (δt) and fast axis direction (ϕ) for individual XKS phases and categorizes them according to their quality as "good," "average," "poor" and "null-measurement." The categorization is based on thresholds for characteristic parameters derived from complementary approaches (Bowman & Ando, 1987; Chevrot, 2000; Silver & Chan, 1991). We refer the reader to the corresponding publication for a more detailed description (Link et al., 2022). Considering all available events and stations, we obtained a total of 21709 splitting measurements. Following the above automated approach, 6453 of the measurements were selected as "good," and 9568 as "average" (Link et al., 2022, see Figure 2a). In total, 5688 measurements showed no splitting and were categorized as "null measurements," which arise if the backazimuth of an event is aligned (near-) parallel to either the fast or the slow direction of an anisotropic layer or in the case of isotropy (see Figure S1 in Supporting Information S1). The lateral distribution of splits is highly diverse due to the nature of the different deployments with permanent stations providing up to 35 years of data and OBS deployments of less than 9 months recording time.

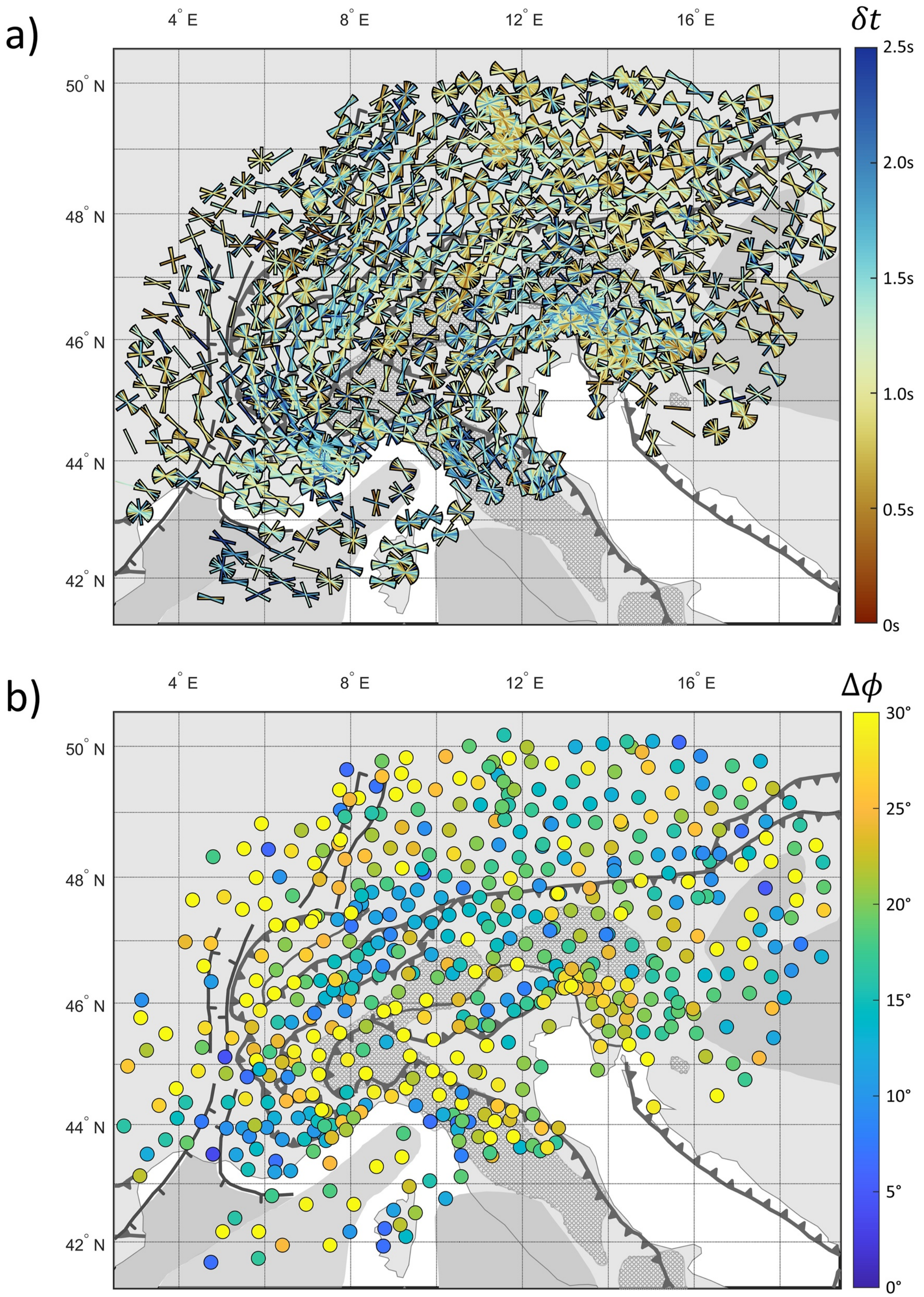

Figure 2. (a) All 16021 splitting-measurements from our shear-wave splitting analysis of the individual core-mantle converted phases observed at the 591 stations in the AlpArray network, plotted at the corresponding station locations. Colored bars are aligned with the fast axis orientations (ϕ) for phases exhibiting clear splitting. The color indicates the delay time (δt). (b) Variability of the measurements, as represented by the standard deviation ($\Delta\phi$) of the non-null measurements for the fast axis orientation at each individual station, where more than three measurements are categorized as good or average. (a and b) The background shows the tectonic features of Figure 1.

10.1029/2023JB027192

2.2. Joint Analysis for One and Two Anisotropic Layers

In the following, we perform a joint splitting analysis to infer the one- or two-layer anisotropic model that best explains the splitting observations for multiple events or phases at a single station (see Homuth et al., 2016; Link et al., 2022; Reiss & Rümpker, 2017; Wolfe & Silver, 1998 for further details). The inclusion of two layers in our analysis is motivated by previously reported layered anisotropy in the broader Alpine region (Link & Rümpker, 2021; Plenefisch et al., 2001; Qorbani et al., 2015; Salimbeni et al., 2008; Vinnik et al., 1994; Walther et al., 2014) and by the observed increase in splitting parameter variation at neighboring stations (see Figure 2b), which suggests the presence of layered anisotropy. Our approach provides effective splitting parameters valid for all phases and serves to mitigate effects of noise or small-scale structural heterogeneities. We assume hexagonal anisotropic media with horizontal fast axes for both layers in our joint splitting analysis, as the near-vertical incidence of the core-mantle converted phases provides limited sensitivity for resolving further complexities. The two (or four) splitting parameters that characterize the one (or two) anisotropic layer(s) are determined by grid search over the complete ranges of fast axes and delay times, with the 'minimization-of-energy' criterion applied to all transverse components simultaneously. The results of the single-layer analysis are shown in Figure 4. A discussion of the results is given further below. Shear-wave splitting analyses in terms of two anisotropic layers are usually based on characteristic (90°-periodicity) back-azimuthal variations of the splitting parameters observed at a single station. However, the joint analysis of all phases used here employs the waveforms directly and, thus, makes use of all available information contained in the full waveform.

In both approaches (for one and two layers), we estimate the uncertainty of the splitting parameters using a bootstrapping approach (Efron, 1979), where we simultaneously minimize the transverse energy for subsets of the phases recorded at a station. Each step in the bootstrapping produces one possible one- or two-layer result (one pair and two pairs of parameters for the one layer and two-layer assumptions, respectively). For the two-layer models, we accept solutions only if the modulo-90° backazimuth values of ϕ in the upper- and lower-layer differ by at least 25°, while both delay times are larger than 0.4 s, and the solution results in a further reduction of the transverse-component energy (after correcting for the splitting) compared to the one-layer joint splitting analysis. The single-layer solution for the station is preferred if no two-layer solution is obtained that improves the data fit. We ultimately obtain 189 stations that show improvement in data fit with two-layer splitting parameters. Analyses for layered anisotropy often suffer from ambiguities in the solution (see Rümpker et al., 2023), which we also observe for parts of our data set. Therefore, the final distribution of the two-layer parameters after bootstrapping is analyzed for spatial clustering (by comparison with neighboring station) to better constrain these ambiguities and their respective uncertainties. This is further discussed in the following subsection.

2.3. Resolving Ambiguities in a Multi-Station Approach

The two-layer splitting analysis can produce ambiguous results when focusing on individual stations only. Here, we resolve this ambiguity with a multi-station approach by comparing the results of neighboring stations and selecting the smoothest spatial distribution of anisotropic layer parameters. This approach is motivated by the assumption, that the Fresnel zones of the core-mantle converted phases at neighboring stations overlap (Alsina & Snieder, 1995) and, therefore, sample similar anisotropic domains, which would result in a rather gradual change of the observed pattern of splitting parameters at neighboring stations.

For this analysis, we perform a stepwise search that minimizes the variation of the splitting parameters at the neighboring stations. Here, the variation is calculated as the normalized sum of the difference between the splitting parameters at neighboring stations:

$$d = \frac{1}{N} \cdot \sum_{j} \sqrt{\sum_{i} \left(s_i - n_{i,j}\right)^2},$$

where $\vec{s} = \left(\delta\hat{t}_1, \sin(2\phi_1), \cos(2\phi_1), \delta\hat{t}_2, \sin(2\phi_2), \cos(2\phi_2)\right)$ and $\vec{n}_j = \left(\delta\hat{t}_{1,j}, \sin(2\phi_{1,j}), \cos(2\phi_{1,j}), \delta\hat{t}_{2,j}, \sin(2\phi_{2,j}), \cos(2\phi_{2,j})\right)$ correspond to the data vectors at the station of interest and the jth station among the N neighboring stations, respectively. The numerical indices in the data vector correspond to the lower and upper layers. We choose to devide the angular parameter, ϕ, into its second order sine and cosine components to accurately account for the true difference between the two sets of splitting parameters, which may occur at the start and the beginning of an angular cycle. For example, consider an upper layer $\phi_1 = 1^{\circ}$ and $\phi_{1,j} = 179^{\circ}$ at a neighboring station.

10.1029/2023JB027192

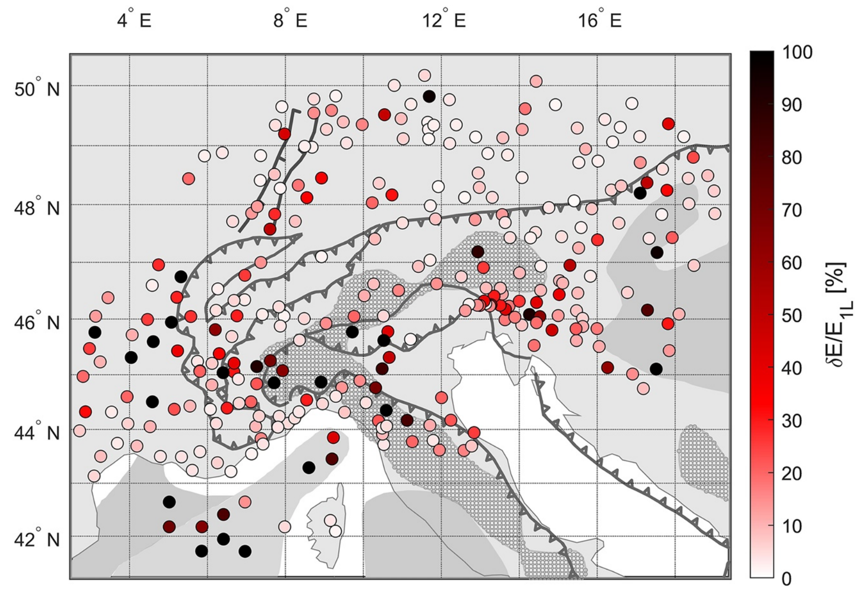

Figure 3. Ratio of the transverse energy that remains after applying the correction for the best fitting two-layer model at each station relative to the one-layer approximation. A positive ratio corresponds to an improvement of the two-layer model versus the one-layer approximation.

The simple difference would be 178°, while the true angular difference between both solutions is 2°, due to the 180°-periodicity of the fast axis direction. Consequently, the angular components vary between −1 and 1 in the data vector, while the delay time varies between 0 and 4s. We normalize the variation parameter, d, to the maximum delay time of 4s to prevent the differences in delay time from exerting a dominating influence.

From several possible (ambiguous) solutions at an individual station, we first select (for all stations) the one that best minimizes the transverse-component energy. Second, we calculate the variation for each possible solution at a randomly selected (reference) station with the best solution at the surrounding stations within a radius of 1°. At the reference station, the solution with the smallest variation is selected. The same procedure is repeated 5000 times for randomly selected stations.

While these stations clearly require the introduction of anisotropic layering to fit the observed shear wave splitting, for the remaining data set it is not as obvious due to limited azimuthal coverage and/or poor data quality. Also note the diversity of the compiled data set containing permanent stations with recordings periods between 2 to more than 30 years of data and temporary stations with recording periods of only 8 months (for OBS stations) up to 36 months (for regular temporary AlpArray land station) resulting in large differences of azimuthal event coverage. As mentioned earlier, we expect that the anisotropic properties are not likely to change drastically over short distances, or that this may not become apparent due to the overlapping Fresnel zones.

Therefore, we also check for the possibility that two anisotropic layers may represent a plausible solution at stations where we previously identified only one layer. To perform this analysis, we fix the orientations in the upper and lower layer based on the results at the neighboring stations (from stations that require two anisotropic layers for optimum data fit) while we allow for variations in delay times of the two layers. We choose to allow for the variation in delay time as previous studies based on Fresnel zone estimates show that delay-time variations occur over a wider area compared to variations in fast axis (e.g., Alsina & Snieder, 1995). This requires more flexibility in the choice of delay time when performing a lateral averaging. We consider the two-layer model as plausible, if the energy minimization for the best fitting parameters is not degraded compared to the single layer solution. As a result, we identify 298 stations for which we obtain plausible two-layer solutions (see Figure 5). The quality of the data fit compared to the single layer models can be estimated from the improvement of the transverse energy minimization, which is at least 10% at 48.3% of all stations with two-layer solutions (see Figure 3). We project the results for upper and lower layers on a regular grid with 0.8° spacing (the average station spacing of the AlpArray network) by calculating the averages of the splitting parameters from the neighboring splitting parameters weighted by their distance to the grid point. This eliminates outliers and emphasizes the

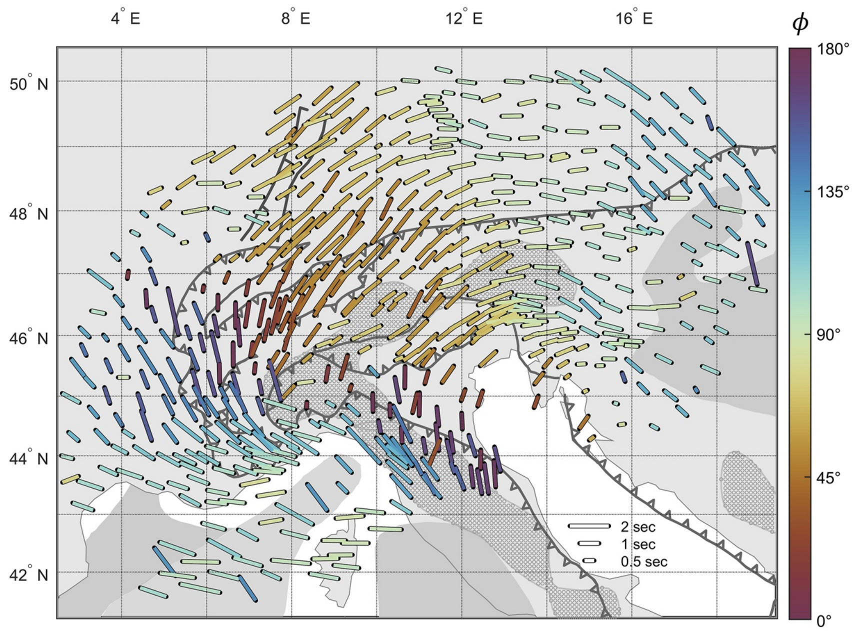

Figure 4. Approximated one-layer anisotropy from joint analysis of shear-wave splitting measurements at the 591 stations of the AlpArray network, plotted at the corresponding station locations. Colored bars denote the fast axis orientations (ϕ) for phases exhibiting clear splitting. The length of the colored bar indicates the delay time (δt) which varies between 0.2 and 2.5 s. The background shows the tectonic features and slab anomalies of Figure 1.

larger-scale anisotropic features (see Figure 6). In this projection, we assign the single layer solutions (at stations not clearly showing two anisotropic layers) to the lower layer, as the deeper layer is likely to represent the asthenospheric anisotropy for the majority of the stations, which is considered to be the dominant source of anisotropy in the upper mantle.

3. Results and Discussion

3.1. Average Splitting Parameters and Layered Anisotropy

In this study, we obtained a total of 16021 splitting measurements and 5688 null-measurements from 591 temporary AlpArray stations, OBS and permanent stations providing a spatially uniform coverage on land and nearby parts of the Ligurian Sea at dense lateral resolution. Individual splitting measurements are characterized by an average delay time, δt, of 1.3 ± 0.6 s. The fast axis direction shows a considerable degree of variation (see Figure 2b). The pattern is not consistent for all stations, as the data set is highly diverse, due to different site and therefore noise conditions, but also due to a large discrepancy in azimuthal coverage resulting from the large difference in recording period. As reported in previous studies for the Central and Eastern Alps (Link & Rümpker, 2021; Qorbani et al., 2015), single measurements of ϕ exhibit a characteristic azimuthal variation, indicative of depth-variations in anisotropy but we also detect significant azimuthal variability in the westernmost Alps and in the Apenninic orogenic belt.

The one-layer approximation of anisotropy obtained from our joint splitting analysis agrees with previous studies, but our station coverage is more dense within the greater Alpine region and further includes the Ligurian Sea (see Figure 4).

Despite the close similarity of the orientation of the splitting and the strike of the mountain chain, the "toroidal" pattern around the Eurasian slab anomaly from the Central Alps around the Western Alps, previously, has been attributed to asthenospheric flow introduced by the retreat of the Apenninic slab (Barruol et al., 2004; Bokelmann et al., 2013; Lucente et al., 2006). The same mechanism was suggested to cause the pattern in the Liguro-Provençal Basin and SE-France (Barruol et al., 2004; Lucente et al., 2006; Margheriti et al., 1996; Salimbeni et al., 2008). A more active role of the Alpine slab had been suggested as an alternative model for the Central Alpine area, producing an evasive flow either due to a retreat or sinking of the slab (Barruol et al., 2011; Petrescu et al., 2020).

10.1029/2023JB027192

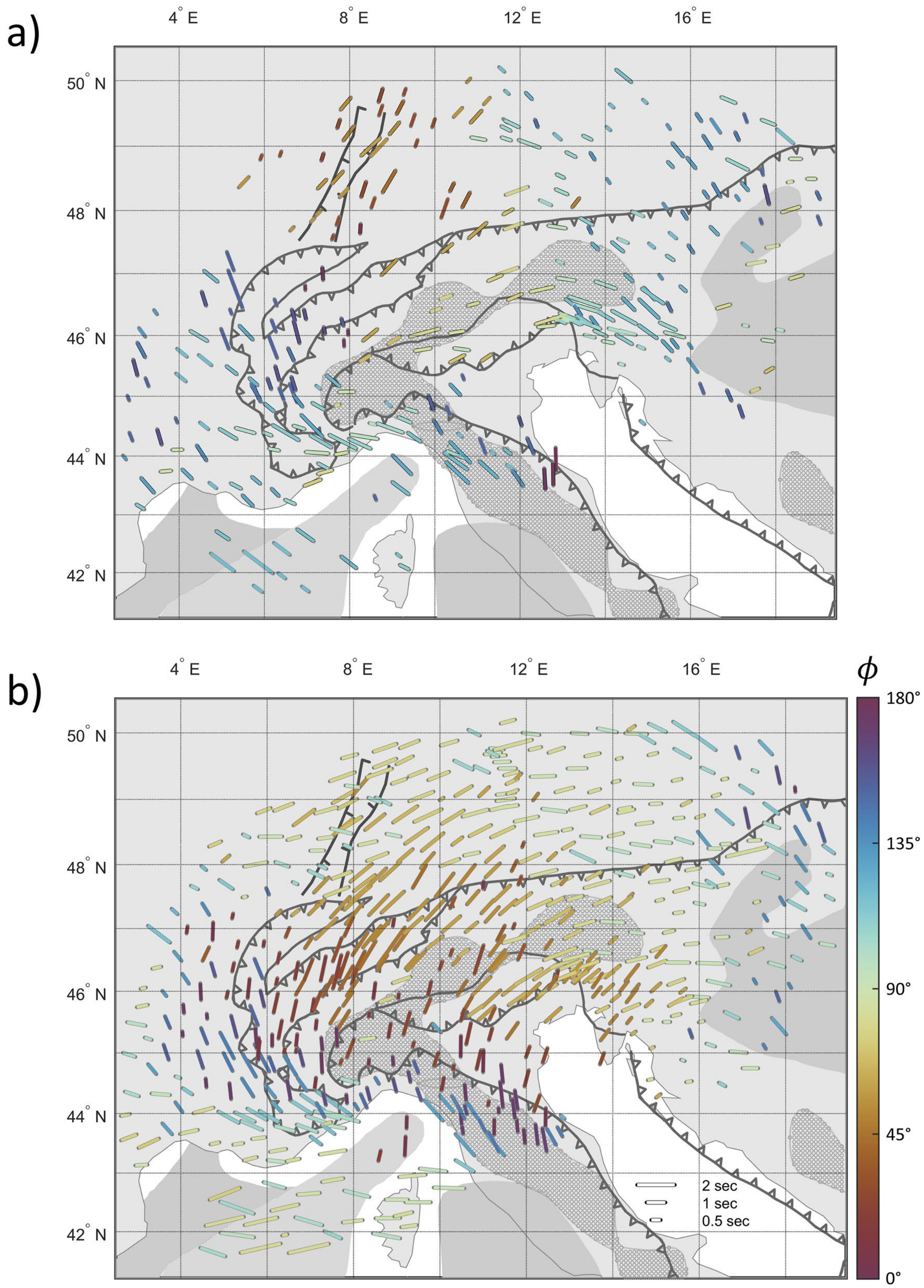

Figure 5. Parameters of the anisotropic layers beneath the Alps and neighboring regions as obtained from a station-based joint splitting analysis for two layers. Bars denote the fast axis orientations (ϕ) in the upper (a) and lower (b) layers; The color indicates the fast axis direction of the final solution and bar length corresponds to the delay time (δt) in that layer. For stations where no two-layer solution was identified, single-layer solutions are assigned to the lower layer. The background shows the tectonic features and slab anomalies of Figure 1.

10.1029/2023JB027192

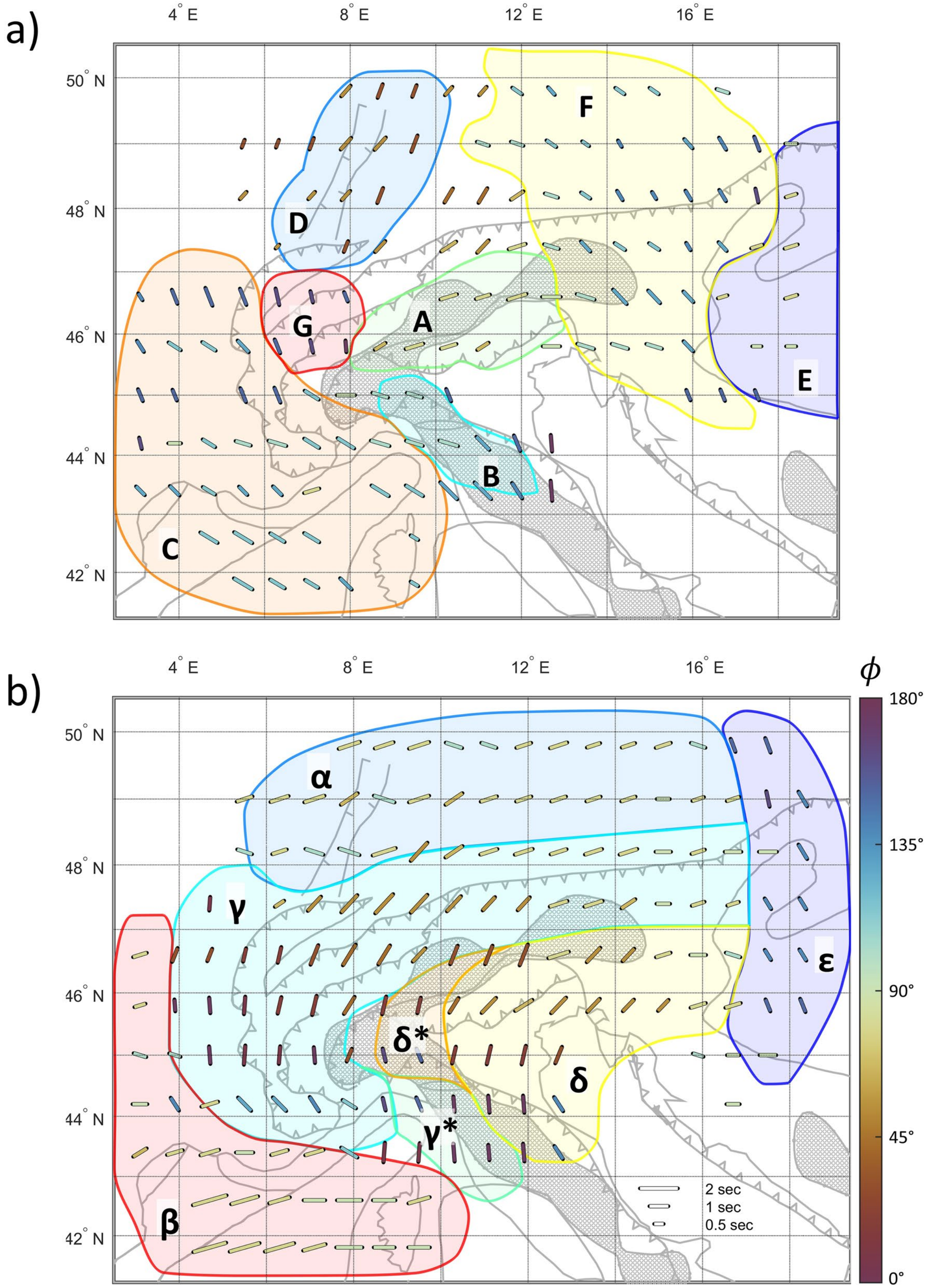

Figure 6. Parameters of the two anisotropic layers beneath the Alps and neighboring regions as obtained from regional averages of our two-layer splitting analysis (Figure 5). Bars denote the fast axis orientations (ϕ) in the upper (a) and lower (b) layers for averages on an equally spaced interpolated grid, and bar length corresponds to the delay time (δt) in that layer. The parameters interpreted as corresponding to distinct tectonic processes (as described in the main text) are grouped in the areas labeled A to G for the upper layer and α to ε for the lower layer. The background shows the tectonic features and slab anomalies of Figure 1.

10.1029/2023JB027192

The transition to the Eastern Alps with a clockwise rotation from EW to about 120° was interpreted as flow following the extension of the Pannonian Basin (Bokelmann et al., 2013). The anisotropy beneath the Adriatic plate has been found to be quite complex despite the small volume the patterns occur (Petrescu et al., 2020; Salimbeni et al., 2013) with an evasive asthenospheric flow behind the Adriatic slab and larger scale NS-flow rotating into EW-direction in vicinity of the Alpine slab blocking the NS flow.

In summary, most of the overall pattern has been attributed to asthenospheric flow implying that the deformation caused in the lithosphere produces negligible contribution to the measured shear-wave splitting. However, our joint splitting analysis for two anisotropic layers throughout the broader Alpine region presents strong evidence for layered anisotropy. This expands upon the previously reported indications for layered anisotropy (Link & Rümpker, 2021; Plenefisch et al., 2001; Qorbani et al., 2015; Salimbeni et al., 2008; Vinnik et al., 1994; Walther et al., 2014) suggesting that additional information about the asthenosphere/lithosphere system can be extracted from shear-wave splitting. We will discuss the implications further in the following.

3.2. The Role of Asthenospheric Flow and Lithospheric Deformation

From the joint splitting analysis, we find that a considerable number (189) of AlpArray stations exhibit splitting parameters with clear indication for anisotropic layering as the transverse component energy reduction is significantly improved by considering two anisotropic layers. The test for plausible two-layer solutions (as described above) shows that two-layer anisotropy can explain the splitting observations at even more stations (298 of the 591 analyzed, see Figure 5).

To emphasize the larger scale pattern and improve visibility, we project the results to a regular grid of 0.8° spacing, which also serves to eliminate outliers. We group the splitting parameters into seven regions for the upper layer and five regions for the lower layer that show coherent anisotropic parameters and suggest common tectonic processes (groups A to G for the upper layer and α to ε for the lower layer in Figures 6a and 6b, respectively) related to the Alpine orogenesis and further tectonic processes in the surrounding areas.

3.2.1. Upper Layer Anisotropy

Upper layer anisotropy of region A and B show parallel fast axis orientation with the strike of the Eurasian and Adriatic slabs, but also align with the major sutures and faults indicating a lithospheric origin of deep reaching faults, that connect surface deformation with depth. The parallel orientation has been observed previously for the Eurasian lithosphere beneath the Alpine orogeny (Link & Rümpker, 2021; Qorbani et al., 2015) as well as for the Adriatic lithosphere beneath the Apennines (Plomerová et al., 2006). However, this pattern is confined to the orogenic region and there is lack of evidence, that this fabric continues further North into the Eurasian lithosphere. Therefore, a connection of deformation due to collision and the development of the lithospheric fabric normal to the compression appears likely.

This mechanism has been suggested for the orogen parallel anisotropy beneath the Apennines as well (Margheriti et al., 1996) with an alignment of anisotropic fabric along strike of the orogenic belt due to the deformation introduced by still active compression within the lithosphere. In addition, a shallow asthenospheric flow within the mantle wedge might contribute to the measured parallel direction caused by suction of the still ongoing retreat of the Calabrian slab to the South-East. The Adriatic subduction is characterized by a retreating slab, which causes the compression within the Adriatic plate, while this retreat results in strong extension at the same time in the back-arc confining the region C. As suggested, this retreat leads to an alternative scenario for the belt-parallel anisotropy explaining its close vicinity to the Adriatic slab, as it introduces an evasive mantle flow parallel to its boundary (Salimbeni et al., 2013). The Liguro-Provençal Basin (southern part of region C) shows an anisotropy, which is aligned with the direction of extension with close to normal orientation relative to the strike of the Apennines (Lucente et al., 2006). Interestingly, the pattern of parallel fast axis in the upper layer continues further to the North-West into the Eurasian lithosphere beneath SE France indicating a continuation of the extensional stress in the lithosphere. Previous studies suggested a shallow asthenospheric flow into the directions found in the upper layer for SE France, which is introduced by the retreat of the Adriatic slab (Barruol et al., 2004; Barruol & Granet, 2002; Lucente et al., 2006). However, the results from our study imply the presence of two distinct anisotropic regions at depth, with the upper layer oriented in extension direction. Developing such vertically distinct anisotropy within the asthenosphere appears unlikely, while a reorientation of the fabric at shallow levels of the asthenosphere due to the retreat might very well cause such a layering. Future studies with a more direct way of inferring the depth of the anisotropic origin (e.g., Chevrot, 2006; Mondal & Long, 2019) might have the potential to clarify this uncertainty.

In region D, we find upper layer anisotropy clustered in the vicinity of the Rhine graben and find parallel directions of the anisotropy with its strike. These observations agree with the recently discovered complexity in the splitting measurements at station BFO (Ritter et al., 2022). The authors report on indication for layered anisotropy, similar to our findings, and short-scale lateral variations. Their study underlines the importance of long-term seismic deployments to reliably recover lithospheric and asthenospheric structures in continental lithosphere, which is also a significant condition for the successful application of our multi-station approach. However, there is no evidence for a larger scale impact of this feature to the overall mantle dynamics in the region and no direct connection to the subduction system. For the interpretation of shear-wave splitting measurements, this lithospheric feature is important to incorporate in the analysis to recover the mantle flow pattern beneath (see lower layer region γ).

Region E coincides with the location of the Pannonian Basin, which developed in the retreat of the Eurasian slab resulting in the development of the Carpathian orogeny and the extension of the Pannonian Basin (Faccenna et al., 2014). The fast axis direction parallels the main extension direction similar to the observation beneath the Liguro-Provençal Basin in region C.

The anisotropic pattern of region F differs from the remaining observations as the fast axis direction shows no alignment with tectonic features cross-cutting major sutures and the Eurasian slab anomaly beneath the Eastern Alps. This is a strong indication for a shallow asthenospheric origin. The anisotropic pattern of region F crosscuts several tectonic features across the Eastern Alps including the Eurasian slab beneath the Eastern Alps, which had been identified with the location of a possible slab gap in previous studies. The fast axis is oriented NW-SE and extends to a larger area to the East, which indicates a shallow asthenospheric origin. This zone includes a previously proposed lateral gap in the Eurasian slab that developed from a break-off event (Kästle et al., 2020; Link & Rümpker, 2021), enabling a reorientation of (shallow) asthenospheric flow through the gap, which provides a channel for the flow of mantle material north of the Eurasian slab toward the actively retreating Aegean slab. The alignment of the upper-layer ϕ with the single-layer solutions farther to the east indicates such a systematic change in the mechanism causing mantle flow, described as follows. The Aegean subduction zone to the southeast of the Alpine orogeny may be responsible for the larger-scale fast axis orientation (mostly in the upper layer, but also continued in the lower layer pattern of region ε beneath the Pannonian Basin). The retreat of the Aegean slab could cause a suction force, thereby dragging mantle material from the Alpine foreland to the southeast. The fast axis also aligns with the Trans-European Suture Zone, which marks the edge of the Eurasian craton (Pharaoh et al., 2006), whose thick lithosphere (Geissler et al., 2010; Plomerová & Babuška, 2010) could guide the flow driven by the retreating Aegean slab.

Region G crosscuts tectonic sutures similar to region F, which might indicate a shallow asthenospheric contribution as well, possibly indicating an ongoing break-off of the Eurasian slab in the Western Alps similarly to the further advanced break-off beneath the Eastern Alps.

3.2.2. Lower Layer Anisotropy

The lower layer (Figure 6b) appears to show slightly less clear separation of anisotropic regions with coherent patterns. This is to be expected, as the area which affects the splitting increases laterally with depth (Rümpker & Ryberg, 2000). As a result, the measured splitting shows an integrated effect over a larger area, which appears as a smoothing of the overall pattern observed in the lower layer. Generally, we expect the lower layer to represent asthenospheric mantle flow, which can be assumed to provide the major contribution to the observed shear-wave splitting (Long & Becker, 2010; Silver, 1996). It, therefore, seems plausible to assign the single layer anisotropic parameters to the lower layer in our interpretation.

Regions α and β at the northern and eastern boundary region with larger distance to the slab systems beneath the Alpine and Apennine suture zones, show a consistent E-W direction of fast axis orientation. This pattern is interrupted sharply by a parallel orientation of the fast axis shown in region γ and γ*. An equivalent pattern is found on both sides of the slab systems considering the parallel fast axis orientation also seen in region δ and δ*. The eastern boundary of the study region, ε, shows again an interruption of the parallel fast axis with the strike of the slab system and parallels NW-SE with the fast axis direction of the upper layer of region F indicating a continuation of the shallow asthenospheric flow at larger depth beneath the Pannonian Basin. The EW directed mantle flow in region β as well as the transition to a NW-SE directed flow further to the East is to be expected

10.1029/2023JB027192

as shown from mantle flow models for the greater Mediterranean region (Faccenna et al., 2014). However, from dynamic modeling, the transition of these directions is expected to be smooth and to occur further East relative to the sharp transition that we find here. The collocation of the transition with the slab gap beneath the Eastern Alps indicates an important role of the Eurasian slab as barrier for the expected mantle flow forcing the transition to the NW-SE oriented flow to its Eastern end (with exception of the channeled flow through a gap beneath the Eastern Alps, see upper layer anisotropy in region F). For the mantle flow in closer vicinity to the slab system (regions γ and δ), the Eurasian slab appears to take a passive role as well, acting as a barrier and channeling the mantle flow (Barruol et al., 2004). In contrast, the flow is mainly driven by the retreat of the Adriatic slab to its current position beneath the Apennines (Barruol et al., 2004; Faccenna et al., 2014; Lucente et al., 2006; Margheriti et al., 1996). This produces a suction force, due to a mass deficit in front of the Apenninic slab, which draws material from the larger surrounding area toward the front of the Adriatic slab. This manifests as an apparent toroidal flow around the Western edge of the Eurasian slab (Barruol et al., 2011; Bokelmann et al., 2013; Hein et al., 2021; Petrescu et al., 2020). The equivalent fast axis orientation behind the Adriatic slab and in front of the Euasian slab, beneath the Adriatic plate results from the evasive mantle flow driven by the retreating Adriatic slab as well (Király et al., 2018). As already shown previously (Salimbeni et al., 2013), the anisotropy shows subparallel to oblique directions relative to the strike of the Adriatic slab, while a parallel direction would be expected for this model. The retreat of the Eurasian slab beneath the Carpathians at an earlier stage and later of the Aegean slab might introduce an additional force drawing the material beneath the Adriatic plate toward the front of these slabs. The superposition of these forces could explain the rotation of the fast axis beneath the Adriatic plate that is observed. The geometry of the Eurasian and Dinaric slab in the South-East forces the mantle to flow in a strong rotational pattern as seen in region delta from a NS orientation in the South to EW orientation (to NNW-SSE) in the Central-Western part.

3.3. Sequence of Tectonic Events in the European Alps

Our analysis of two layers of anisotropy based on shear-wave splitting measurements from the AlpArray data set allows an interpretation of the relevant tectonodynamic processes beneath the European Alps that is significantly more detailed than those previously reported. The results further highlight how vertical resolution of anisotropy allows insight into the sequence of the complex tectonic processes in the region. In the following, we relate the anisotropic patterns to the tectonic processes that occur in the Central Mediterranean region, as described by Faccenna et al. (2014).

The east-west directed anisotropy in larger distance to the orogeny is sharply interrupted by anisotropic patterns that can be attributed to specific tectonic processes. Therefore, it is likely that this background flow predates the Eurasian-Adriatic continental collision at around 35 Ma (see Figure 7a). With the rollback of the Adriatic slab and the corresponding opening of the Liguro-Provençal Basin (starting ∼30–35 Ma) the lithosphere of the Basin experiences strong extensional strain and develops lithospheric anisotropy with a symmetry axis aligning with the strain direction. Due to the role back, the evasive mantle flow behind the Adriatic slab and the compensational flow behind the Eurasian slab starts to develop (Figure 7b). As the geometry of the Adriatic subduction changes, compensational and evasive flows adjust within the dynamic system. Consequently, the mantle flow is channeled by the steep slabs in the subduction system (see Figures 7b–7f). With the rollback of the easternmost part of the Eurasian slab starting at around 22 to 20 Ma, the Pannonian Basin as well as the Carpathian orogeny develop, which produce strain in the lithospheric mantle in the Basin area. This leads, similar to the Liguro-Provençal Basin, to anisotropy in the lithosphere parallel to the extension direction (Figure 7c). The eastward retreat of the Eurasian slab beneath the Carpathians causes segmentation and allows mantle to flow southward toward the Aegean slab, which initiated its retreat parallel to the Adriatic slab ∼30–35 Ma (see Figures 7d and 7b, respectively). It has been suggested, that the break-off of the eastern Eurasian slab is concurrent with the opening of the Pannonian Basin (Kästle et al., 2020), which allows shallow asthenospheric flow through a gap in the Eurasian slab toward the Aegean retreating slab. The retreat of the Adriatic slab and the Aegean slab continue until they reach their present-day geometry.

4. Conclusions

We analyzed the complete Alpine range for evidence of layered seismic anisotropy in the upper mantle using shear-wave splitting measurements at 591 seismic stations in an area covered by the AlpArray experiment. We find that layered anisotropy is required to fit the splitting data at 189 of the analyzed stations; layered anisotropy provides a plausible model for the splitting observations at 289 out of the 591 stations. The distinct coherent

Journal of Geophysical Research: Solid Earth

10.1029/2023JB027192

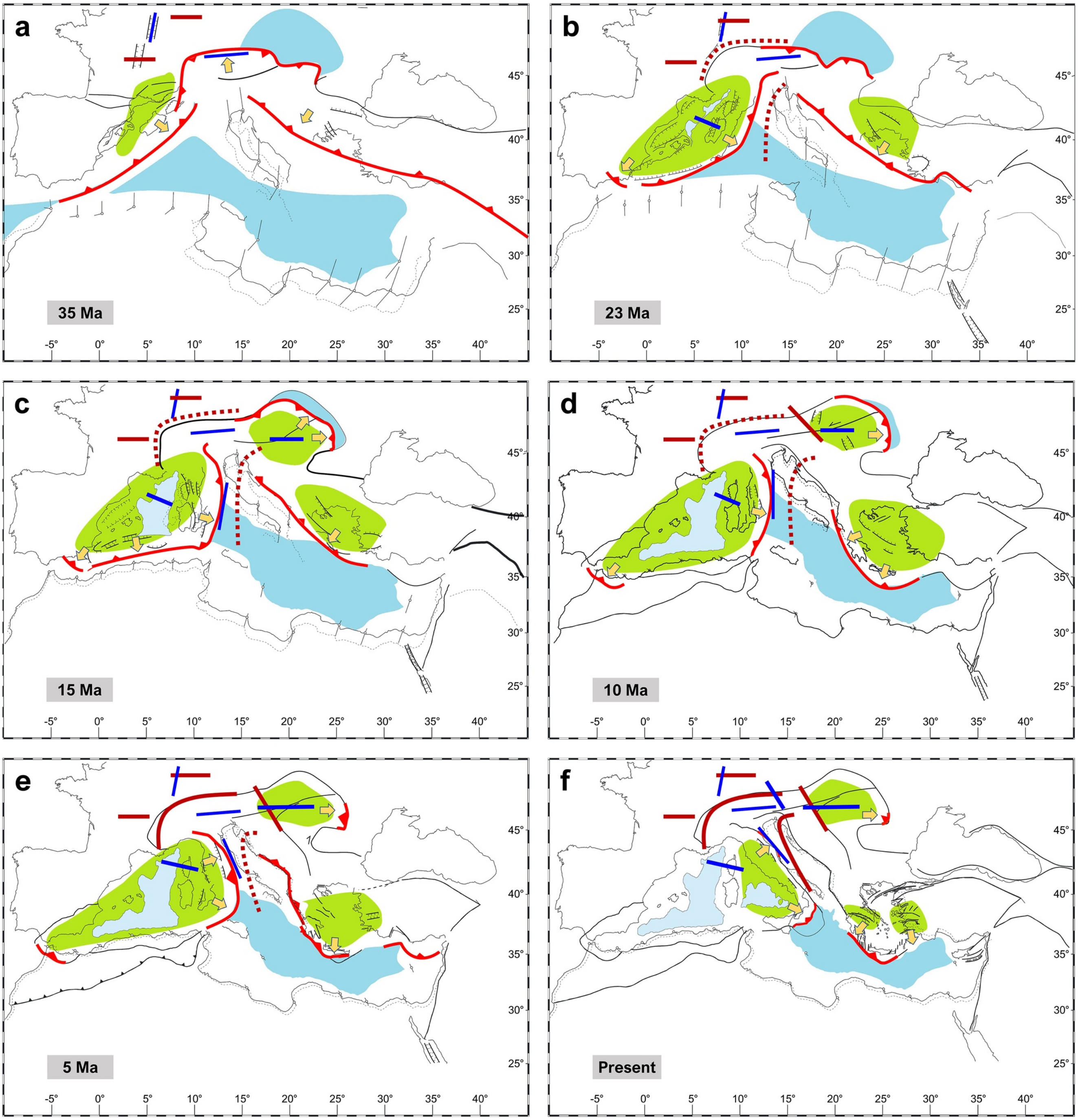

Figure 7. Model of the tectonic history of the Central Mediterranean system from 35 Ma (a) to present (f), based on Faccenna et al. (2014) and the results from anisotropic layering presented here. Dashed and solid lines (red and blue) represent anisotropic patterns originating at the depicted location during the time shown in the panel. Red and blue colors indicate lower- and upper-layer anisotropy, respectively. Solid lines indicate stable anisotropy from its first occurrence to the present, while dashed lines indicate a dynamic change corresponding to tectonic evolution. The red lines with arrows outline active sections of the trenches. Yellow arrows denote compression or extensional directions. Green color highlights areas of extension, while light blue areas indicate oceanic lithosphere.

patterns of the layered anisotropy allow us to identify subsequent processes in the Mediterranean tectonics from which the lithospheric and asthenospheric anisotropy originated.

Our findings suggest that the mantle dynamics exert a strong influence on the tectonism in this region. For example, east-west mantle flow occurs for the greater area beneath Western Europe, extending into the Alpine-Apenninic area, while the Aegean slab imposes a drag force on the mantle in the east. The Eurasian slab appears as a strong barrier and channels the mantle flow initiated by the dragging force of the retreating Adriatic and Aegean slabs. These inferences may also have significant consequences for establishing appropriate boundary conditions in geodynamic models of the Alpine orogeny.

The inferred layering of the anisotropy in the Alpine area provides clear evidence for lithospheric anisotropy in the extensional basins, such as the Liguro-Provençal and Pannonian, Basins, the Rhine graben, and in the compressional regimes of the Alpine and Apenninic orogeny. This indicates that shear wave splitting results not only from asthenospheric flow, as previously interpreted, but is also influenced by the complex tectonic history recorded in the lithosphere. However, uncertainty persists regarding the relative allocation of anisotropy between lithosphere and asthenosphere due to the limited depth resolution of the applied techniques. Further investigations using more direct methods to infer the depth of anisotropic fabric could potentially clarify this uncertainty (e.g., Chevrot, 2006; Mondal & Long, 2019).

We analyzed splitting from SKS- as well as SKKS-phases and found strong splitting in both. In principle, these phases would allow for an analysis of deep mantle anisotropy based on discrepancies in their splitting parameters (e.g., Grund & Ritter, 2019; Long & Lynner, 2015; Wolf et al., 2019). A future study aiming on differentiating between these two phases measured for the same events holds potential to the discovery of deep mantle structure.

Acknowledgments
We would like to thank our colleagues Miriam Christina Reiss, Ayoub Kaviani and Michael Lindenfeld for their helpful comments in finalizing this manuscript. An earlier version of this manuscript has been edited with the support of the Nature Research Editing Service. We are grateful for the constructive criticism and helpful suggestions provided by previous and current reviewers. We acknowledge the operation of the AlpArray seismic network (Z3) and the permanent seismic networks used in this study: BW: Department of Earth and Environmental Sciences, Geophysical Observatory, University of München; CH: Swiss Seismological Service (SED) at ETH Zurich; CR: University of Zagreb; CZ: Charles University in Prague (Czech), Institute of Geonics (IGN), Institute of Geophysics, Academy of Sciences of the Czech Republic, Institute of Physics of the Earth Masaryk University (Czech), Institute of Rock Structure and Mechanics (IRSM AS CR); FR: RESIF; G: Institut de Physique du Globe de Paris; GE: GEOFON Program (GFZ-Potsdam, Germany); GR: BGR Federal Institute for Geosciences and Natural Resources (BGR, Germany); GU: University of Genoa (UniGe); HU: Geodetic and Geophysical Research Institute (Hungary); IU: Albuquerque Seismological Laboratory (ASL)/USGS; IV, MN,: INGV Seismological Data Centre; NI: OGS (Istituto Nazionale di Oceanografia e di Geofisica Sperimentale) and University Of Trieste; OE: ZAMG-Zentralanstalt für Meterologie und Geodynamik; OX: OGS (Istituto Nazionale di Oceanografia e di Geofisica Sperimentale); RD: Departement d'Analyse et Surveillance de l'Environnement du CEA; RF: University of Trieste; SI: ZAMG—Central Institute for Meteorology and Geodynamics; SK: Geophysical Institute, Slovak Academy of Sciences; SL: Slovenian Environment Agency, ST: Geological Survey-Provincia Autonoma di Trento. We would also like to acknowledge the efforts of ORFEUS, EIDA and IRIS for providing the accessibility to the seismic data sets. We further acknowledge the scientific exchange and cooperation within the AlpArray Working Group (http://www.alparray.ethz.ch) and would like to thank the entire AlpArray Seismic Network Team: György HETÉNYI, Rafael ABREU, Ivo ALLEGRETTI, Maria-Theresia APOLONER, Coralie AUBERT, Simon BESANÇON, Maxime BÈS DE BERC, Götz BOKELMANN, Didier BRUNEL, Marco CAPELLO, Martina ČARMAN, Adriano CAVALIERE, Jérôme CHÈZE, Claudio CHIARABBA, John CLINTON, Glenn COUGOULAT, Wayne C. CRAWFORD, Luigia CRISTIANO, Tibor CZIFRA, Ezio D'ALEMA, Stefania DANESI, Romuald DANIEL, Anke DANNOWSKI, Iva DASOVIĆ, Anne DESCHAMPS, Jean-Xavier DESSA, Cécile DOUBRE,

Data Availability Statement

All seismic data of the permanent and temporary stations within the AlpArray initiative (Z3: AlpArray Seismic Network, 2015; BW: Department of Earth and Environmental Sciences, Geophysical Observatory, University of Munchen, 2001; CH: Swiss Seismological Service (SED) At ETH Zurich, 1983; CR: University of Zagreb, 2001; CZ: Charles University in Prague (Czech) et al., 1973; FR: RESIF, 1995; G: Institut de physique du globe de Paris (IPGP) & École et Observatoire des Sciences de la Terre de Strasbourg (EOST), 1982; GE: GEOFON Data Centre, 1993; GR: Federal Institute for Geosciences and Natural Resources, 1976; GU: University of Genoa, 1967; HU: Kövesligthy Radó Seismological Observatory (Geodetic And Geophysica Institute, Research Centre For Astronomy And Earth Sciences, Hungarian Academy Of Sciences (MTA CSFK GGI KRSZO)), 1992; IU: Albuquerque Seismological Laboratory/USGS, 2014; IV: Istituto Nazionale di Geofisica e Vulcanologia (INGV), 2005; MN: MedNet Project Partner Institutions, 1990; NI: OGS (Istituto Nazionale di Oceanorafia e di Geofisica Sperimentale) & Universit of Trieste, 2002; OE: ZAMG—Zentralanstalt für Meterologie und Geodynamik, 1987; OX: Istituto Nazionale di Oceanografia e di Geofisica Sperimentale—OGS, 2016; RD: RESIF, 2018; RF: University of Trieste, 1993; SI: Istituto Nazionale di Geofisica e Vulcanologia (INGV), 2006; SK: ESI SAS, 2004; SL: Slovenian Environment Agency, 1990; ST: Geological Survey-Provincia Autonoma di Trento, 1981) can be downloaded from ORFEUS-databases which is part of EIDA, the European Integrated Data Archive. The automatic version of SplitRacer is a publicly available software package (Link et al., 2022) used for most parts of the data processing and analysis as described above. The results of the individual splitting as well as the layered anisotropic model is available alongside this publication as Supporting Information S1. The individual and average splitting parameters are further made available in the shear wave splitting database provided by IRIS and Université de Montpellier, Laboratoire Géosciences (Barruol et al., 2009).

References

Albuquerque Seismological Laboratory/USGS. (2014). Global seismograph network (GSN—IRIS/USGS) [Dataset]. International Federation of Digital Seismograph Networks. https://doi.org/10.7914/SN/IU

AlpArray Seismic Network. (2015). AlpArray seismic network (AASN) temporary component, AlpArray working group [Dataset]. Other/Seismic Network. https://doi.org/10.12686/alparray/z3_2015

Alsina, D., & Snieder, R. (1995). Small-scale sublithospheric continental mantle deformation: Constraints from SKS splitting observations. *Geophysical Journal International*, *123*(2), 431–448. https://doi.org/10.1111/j.1365-246X.1995.tb06864.x

Barruol, G., Bonnin, M., Pedersen, H., Bokelmann, G. H. R., & Tiberi, C. (2011). Belt-parallel mantle flow beneath a halted continental collision: The Western Alps. *Earth and Planetary Science Letters*, *302*(3–4), 429–438. https://doi.org/10.1016/j.epsl.2010.12.040

Barruol, G., Deschamps, A., & Coutant, O. (2004). Mapping upper mantle anisotropy beneath SE France by SKS splitting indicates Neogene asthenospheric flow induced by Apenninic slab roll-back and deflected by the deep Alpine roots. *Tectonophysics*, *394*(1–2), 125–138. https://doi.org/10.1016/j.tecto.2004.08.002

Barruol, G., & Granet, M. (2002). A Tertiary asthenospheric flow beneath the southern French Massif Central indicated by upper mantle seismic anisotropy and related to the west Mediterranean extension. *Earth and Planetary Science Letters*, *202*(1), 31–47. https://doi.org/10.1016/S0012-821X(02)00752-5

10.1029/2023JB027192

Sven EGDORF, ETHZ-SED Electronics Lab, Tomislav FIKET, Kasper FISCHER, Wolfgang FRIEDERICH, Florian FUCHS, Sigward FUNKE, Domenico GIARDINI, Aladino GOVONI, Zoltán GRÁCZER, Gidera GRÖSCHL, Stefan HEIMERS, Ben HEIT, Davorka HERAK, Marijan HERAK, Johann HUBER, Dejan JARIĆ, Petr JEDLIČKA, Yan JIA, Hélène JUND, Edi KISSLING, Stefan KLINGEN, Bernhard KLOTZ, Petr KOLÍNSKÝ, Heidrun KOPP, Michael KORN, Josef KOTEK, Lothar KÜHNE, Krešo KUK, Dietrich LANGE, Jürgen LOOS, Sara LOVATI, Deny MALENGROS, Lucia MARGHERITI, Christophe MARON, Xavier MARTIN, Marco MASSA, Francesco MAZZARINI, Thomas MEIER, Laurent MÉTRAL, Irene MOLINARI, Milena MORETTI, Anna NARDI, Jurij PAHOR, Anne PAUL, Catherine PÉQUEGNAT, Daniel PETERSEN, Damiano PESARESI, Davide PICCININI, Claudia PIROMALLO, Thomas PLENEFISCH, Jaroslava PLOMEROVÁ, Silvia PONDRELLI, Snježan PREVOLNIK, Roman RACINE, Marc RÉGNIER, Miriam REISS, Joachim RITTER, Georg RÜMPKER, Simone SALIMBENI, Marco SANTULIN, Werner SCHERER, Sven SCHIPPKUS, Detlef SCHULTE-KORTNACK, Vesna ŠIPKA, Stefano SOLARINO, Daniele SPALLAROSSA, Kathrin SPIEKER, Josip STIPČEVIĆ, Angelo STROLLO, Bálint SÜLE, Gyöngyvér SZANYI, Eszter SZŰCS, Christine THOMAS, Martin THORWART, Frederik TILMANN, Stefan UEDING, Massimiliano VALLOCCHIA, Luděk VECSEY, René VOIGT, Joachim WASSERMANN, Zoltán WÉBER, Christian WEIDLE, Viktor WESZTERGOM, Gauthier WEYLAND, Stefan WIEMER, Felix WOLF, David WOLYNIEC, Thomas ZIEKE, Mladen ŽIVČIĆ and Helena ŽLEBČÍKOVÁ. All figures in this study are produced using the plotting and mapping tools of the MATLAB software, version R2020a. GR acknowledges support from DFG Grants RU 886/13-1 and RU 886/15-1. Open Access funding enabled and organized by Projekt DEAL.

Barruol, G., Wuestefeld, A., & Bokelmann, G. (2009). SKS-Splitting-database [Dataset]. Université de Montpellier, Laboratoire Géosciences. https://doi.org/10.18715/SKS_SPLITTING_DATABASE

Bokelmann, G. H. R., Qorbani, E., & Bianchi, I. (2013). Seismic anisotropy and large-scale deformation of the Eastern Alps. *Earth and Planetary Science Letters*, *383*, 1–6. https://doi.org/10.1016/j.epsl.2013.09.019

Bowman, J. R., & Ando, M. (1987). Shear-wave splitting in the upper-mantle wedge above the Tonga subduction zone. *Geophysical Journal*, *88*(1), 25–41. https://doi.org/10.1111/j.1365-246X.1987.tb01367.x

Charles University in Prague (Czech), Institute of Geonics, Institute of Geophysics, Academy of Sciences of the Czech Republic, Institute of Physics of the Earth Masaryk University (Czech), & Institute of Rock Structure and Mechanics. (1973). Czech regional seismic network [Dataset]. International Federation of Digital Seismograph Networks. https://doi.org/10.7914/SN/CZ

Chevrot, S. (2000). Multichannel analysis of shear wave splitting. *Journal of Geophysical Research*, *105*(B5), 21579–21590. https://doi.org/10.1029/2000JB900199

Chevrot, S. (2006). Finite-frequency vectorial tomography: A new method for high-resolution imaging of upper mantle anisotropy. *Geophysical Journal International*, *165*(2), 641–657. https://doi.org/10.1111/j.1365-246X.2006.02982.x

Department of Earth and Environmental Sciences, Geophysical Observatory, University of Munchen. (2001). BayernNetz [Dataset]. International Federation of Digital Seismograph Networks. https://doi.org/10.7914/SN/BW

Dewey, J., Helman, M., Knott, S., Turco, E., & Hutton, D. (1989). Kinematics of the western Mediterranean. *The Geological Society of London*, *45*(1), 265–283. https://doi.org/10.1144/GSL.SP.1989.045.01.15

Dewey, J. F., Pitman, W. C. P., III., Ryan, W. B. F., & Bonnin, J. (1973). Plate tectonics and the evolution of the Alpine system. *Geological Society of America Bulletin*, *84*(10), 3137–3180. https://doi.org/10.1130/0016-7606(1973)84<3137:PTATEO>2.0.CO;2

Efron, B. (1979). Bootstrap methods: Another look at the jackknife. *Annals of Statistics*, *7*(1), 1–26. https://doi.org/10.1007/978-1-4612-4380-9_41

ESI SAS. (2004). National network of seismic stations of Slovakia [Dataset]. GFZ Data Services. https://doi.org/10.14470/FX099882

Faccenna, C., Becker, T. W., Auer, L., Billi, A., Boschi, L., Brun, J. P., et al. (2014). Mantle dynamics in the Mediterranean. *Reviews of Geophysics*, *52*(3), 283–332. https://doi.org/10.1002/2013RG000444

Faccenna, C., Piromallo, C., Crespo-Blanc, A., Jolivet, L., & Rossetti, F. (2004). Lateral slab deformation and the origin of the western Mediterranean arcs. *Tectonics*, *23*(1), TC1012. https://doi.org/10.1029/2002TC001488

Federal Institute for GeosciencesNatural Resources. (1976). German regional seismic network (GRSN) [Dataset]. Bundesanstalt für Geowissenschaften und Rohstoffe. https://doi.org/10.25928/mbx6-hr74

Geissler, W. H., Sodoudi, F., & Kind, R. (2010). Thickness of the central and eastern European lithosphere as seen by S-receiver functions. *Geophysical Journal International*. https://doi.org/10.1111/j.1365-246X.2010.04548.x

GEOFON Data Centre. (1993). GEOFON seismic network [Dataset]. Deutsches GeoForschungsZentrum GFZ. https://doi.org/10.14470/TR560404

Geological Survey-Provincia Autonoma di Trento. (1981). Trentino seismic network [Dataset]. International Federation of Digital Seismograph Networks. https://doi.org/10.7914/SN/ST

Grund, M., & Ritter, J. R. R. (2019). Widespread seismic anisotropy in Earth's lowermost mantle beneath the Atlantic and Siberia. *Geology*, *47*(2), 123–126. https://doi.org/10.1130/G45514.1

Handy, M. R., Schmid, S. M., Bousquet, R., Kissling, E., & Bernoulli, D. (2010). Reconciling plate-tectonic reconstructions of Alpine Tethys with the geological–geophysical record of spreading and subduction in the Alps. *Earth-Science Reviews*, *102*(3–4), 121–158. https://doi.org/10.1016/j.earscirev.2010.06.002

Handy, M. R., Ustaszewski, K., & Kissling, E. (2015). Reconstructing the Alps–Carpathians–Dinarides as a key to understanding switches in subduction polarity, slab gaps and surface motion. *International Journal of Earth Sciences*, *104*, 1–26. https://doi.org/10.1007/s00531-014-1060-3

Hein, G., Kolínský, P., Bianchi, I., Bokelmann, G., Hetényi, G., Abreu, R., et al. (2021). Shear wave splitting in the Alpine region. *Geophysical Journal International*, *227*(3), 1996–2015. https://doi.org/10.1093/gji/ggab305

Hetényi, G., Molinari, I., Clinton, J., Bokelmann, G., Bondár, I., Crawford, W. C., et al. (2018). The AlpArray seismic network: A large-scale European experiment to image the Alpine orogen. [Dataset]. Surveys in Geophysics, *39*, 1009–1033. https://doi.org/10.1007/s10712-018-9472-4

Homuth, B., Löbl, U., Batte, A. G., Link, K., Kasereka, C. M., & Rümpker, G. (2016). Seismic anisotropy of the lithosphere/asthenosphere system beneath the Rwenzori region of the Albertine Rift. *International Journal of Earth Sciences*, *105*(6), 1681–1692. https://doi.org/10.1007/s00531-014-1047-0

Institut de physique du globe de Paris (IPGP), & École et Observatoire des Sciences de la Terre de Strasbourg (EOST). (1982). GEOSCOPE, French Global Network of broad band seismic stations [Dataset]. Institut de physique du globe de Paris (IPGP). https://doi.org/10.18715/GEOSCOPE.G

Istituto Nazionale di Geofisica e Vulcanologia (INGV). (2006). Sudtirol network, Italy [Dataset]. Istituto Nazionale di Geofisica e Vulcanologia (INGV). Retrieved from https://terremoti.ingv.it/en/instruments/network/SI

Istituto Nazionale di Geofisica e Vulcanologia (INGV). (2005). Rete Sismica Nazionale (RSN) [Dataset]. Istituto Nazionale di Geofisica e Vulcanologia (INGV). https://doi.org/10.13127/SD/X0FXnH7QfY

Istituto Nazionale di Oceanografia e di Geofisica Sperimentale - OGS. (2016). North-East Italy seismic network [Dataset]. FDSN. https://doi.org/10.7914/SN/OX

Karato, S., Jung, H., Katayama, I., & Skemer, P. (2008). Geodynamic significance of seismic anisotropy of the upper mantle: New insights from laboratory studies. *Annual Review of Earth and Planetary Sciences*, *36*(1), 59–95. https://doi.org/10.1146/annurev.earth.36.031207.124120

Kästle, E. D., El-Sharkawy, A., Boschi, L., Meier, T., Rosenberg, C., Bellahsen, N., et al. (2018). Surface wave tomography of the Alps using ambient-noise and earthquake phase velocity measurements. *Journal of Geophysical Research: Solid Earth*, *123*(2), 1770–1792. https://doi.org/10.1002/2017JB014698

Kästle, E. D., Rosenberg, C., Boschi, L., Bellahsen, N., Meier, T., & El-Sharkawy, A. (2020). Slab break-offs in the Alpine subduction zone. *International Journal of Earth Sciences*, *109*(2), 587–603. https://doi.org/10.1007/s00531-020-01821-z

Kennett, B. L. N., & Engdahl, E. R. (1991). Traveltimes for global earthquake location and phase identification. *Geophysical Journal International*, *105*(2), 429–465. https://doi.org/10.1111/j.1365-246X.1991.tb06724.x

Király, Á., Faccenna, C., & Funiciello, F. (2018). Subduction zones interaction around the Adria microplate and the origin of the Apenninic arc. *Tectonics*, *37*(10), 3941–3953. https://doi.org/10.1029/2018TC005211

Kissling, E., Schmid, S. M., Lippitsch, R., Ansorge, J., & Fügenschuh, B. (2006). Lithosphere structure and tectonic evolution of the Alpine arc: New evidence from high-resolution teleseismic tomography. *Geol Soc London*, *32*(1), 129–145. https://doi.org/10.1144/GSL.MEM.2006.032.01.08

Koulakov, I., Kaban, M. K., Tesauro, M., & Cloetingh, S. (2009). P- and S-velocity anomalies in the upper mantle beneath Europe from tomographic inversion of ISC data. *Geophysical Journal International*, *179*(1), 345–366. https://doi.org/10.1111/j.1365-246X.2009.04279.x

Kövesligethy Radó Seismological Observatory (Geodetic And Geophysical Institute, Research Centre For Astronomy And Earth Sciences, Hungarian Academy Of Sciences (MTA CSFK GGI KRSZO)). (1992). Hungarian national seismological network [Dataset]. GFZ Data Services. https://doi.org/10.14470/UH028726

Laubscher, H. P. (1988). The arcs of the western Alps and the northern Apennines: An updated view. *Tectonophysics*, *146*(1–4), 67–78. https://doi.org/10.1016/0040-1951(88)90082-0

Link, F., Reiss, M. C., & Rümpker, G. (2022). An automatized XKS-splitting procedure for large data sets: Extension package for SplitRacer and application to the USArray [Software]. Computers & Geosciences, *158*, 104961. https://doi.org/10.1016/j.cageo.2021.104961

Link, F., & Rümpker, G. (2021). Resolving seismic anisotropy of the lithosphere–asthenosphere in the central/eastern Alps beneath the SWATH-D network. *Frontiers in Earth Science*, *9*. https://doi.org/10.3389/feart.2021.679887

Lippitsch, R. (2003). Upper mantle structure beneath the Alpine orogen from high-resolution teleseismic tomography. *Journal of Geophysical Research: Solid Earth*, *108*(B8), 2376. https://doi.org/10.1029/2002JB002016

Long, M. D., & Becker, T. W. (2010). Mantle dynamics and seismic anisotropy. *Earth and Planetary Science Letters*, *297*(3–4), 341–354. https://doi.org/10.1016/j.epsl.2010.06.036

Long, M. D., & Lynner, C. (2015). Seismic anisotropy in the lowermost mantle near the Perm Anomaly. *Geophysical Research Letters*, *42*(17), 7073–7080. https://doi.org/10.1002/2015GL065506

Lucente, F. P., Margheriti, L., Piromallo, C., & Barruol, G. (2006). Seismic anisotropy reveals the long route of the slab through the western-central Mediterranean mantle. *Earth and Planetary Science Letters*, *241*(3–4), 517–529. https://doi.org/10.1016/j.epsl.2005.10.041

Malinverno, A., & Ryan, W. B. F. (1986). Extension in the Tyrrhenian Sea and shortening in the Apennines as result of arc migration driven by sinking of the lithosphere. *Tectonics*, *5*(2), 227–245. https://doi.org/10.1029/TC005i002p00227

Margheriti, L., Nostro, C., Cocco, M., & Amato, A. (1996). Seismic anisotropy beneath the Northern Apennines (Italy) and its tectonic implications. *Geophysical Research Letters*, *23*(20), 2721–2724. https://doi.org/10.1029/96GL02519

MedNet Project Partner Institutions. (1990). Mediterranean very broadband seismographic network (MedNet) [Dataset]. Istituto Nazionale di Geofisica e Vulcanologia (INGV). https://doi.org/10.13127/SD/fBBBtDtd6q

Mondal, P., & Long, M. D. (2019). A model space search approach to finite-frequency SKS splitting intensity tomography in a reduced parameter space. *Geophysical Journal International*, *217*(1), 238–256. https://doi.org/10.1093/gji/ggz016

Moretti, I., & Royden, L. (1988). Deflection, gravity anomalies and tectonics of doubly subducted continental lithosphere: Adriatic and Ionian seas. *Tectonics*, *7*(4), 875–893. https://doi.org/10.1029/TC007i004p00875

OGS (Istituto Nazionale di Oceanografia e di Geofisica Sperimentale) and University of Trieste. (2002). North-East Italy broadband network [Dataset]. International Federation of Digital Seismograph Networks. https://doi.org/10.7914/SN/NI

Paffrath, M., Friederich, W., Schmid, S. M., Handy, M. R., & the AlpArray and AlpArray-Swath D Working Group (2021). Imaging structure and geometry of slabs in the greater Alpine area—A P-wave travel-time tomography using AlpArray seismic network data. *Solid Earth*, *12*(11), 2671–2702. https://doi.org/10.5194/se-12-2671-2021

Petrescu, L., Pondrelli, S., Salimbeni, S., Faccenda, M., & Group, A. W. (2020). Mantle flow below the central and greater Alpine region: Insights from SKS anisotropy analysis at AlpArray and permanent stations. *Solid Earth*, *11*(4), 1275–1290. https://doi.org/10.5194/se-11-1275-2020

Pharaoh, T. C., Winchester, J. A., Verniers, J., Lassen, A., & Seghedi, A. (2006). The western accretionary margin of the East European craton: An overview. *Geological Society, London, Memoirs*, *32*(1), 291–311. https://doi.org/10.1144/GSL.MEM.2006.032.01.17

Platt, J. P. (2007). From orogenic hinterlands to Mediterranean-style back-arc basins: A comparative analysis. *Journal of the Geological Society*, *164*(2), 297–311. https://doi.org/10.1144/0016-76492006-093

Plenefisch, T., Klinge, K., & Kind, R. (2001). Upper mantle anisotropy at the transition zone of the Saxothuringicum and Moldanubicum in southeast Germany revealed by shear wave splitting. *Geophysical Journal International*, *144*(2), 309–319. https://doi.org/10.1046/j.0956-540X.2000.01316.x

Plomerová, J., & Babuška, V. (2010). Long memory of mantle lithosphere fabric—European LAB constrained from seismic anisotropy. *Lithos*, *120*(1–2), 131–143. https://doi.org/10.1016/j.lithos.2010.01.008

Plomerová, J., Margheriti, L., Park, J., Babuška, V., Pondrelli, S., Vecsey, L., et al. (2006). Seismic anisotropy beneath the Northern Apennines (Italy): Mantle flow or lithospheric fabric? *Earth and Planetary Science Letters*, *247*(1–2), 157–170. https://doi.org/10.1016/j.epsl.2006.04.023

Qorbani, E., Bianchi, I., & Bokelmann, G. (2015). Slab detachment under the Eastern Alps seen by seismic anisotropy. *Earth and Planetary Science Letters*, *409*(1), 96–108. https://doi.org/10.1016/j.epsl.2014.10.049

Reiss, M. C., & Rümpker, G. (2017). SplitRacer: MATLAB code and GUI for semiautomated analysis and interpretation of teleseismic shear-wave splitting. *Seismological Research Letters*, *88*(2A), 392–409. https://doi.org/10.1785/0220160191

RESIF. (1995). RESIF-RLBP French Broad-band network, RESIF-RAP strong motion network and other seismic stations in metropolitan France [Dataset]. RESIF - Réseau Sismologique et géodésique Français. https://doi.org/10.15778/RESIF.FR

RESIF. (2018). CEA/DASE broad-band permanent network in metropolitan France [Dataset]. RESIF - Réseau Sismologique et géodésique Français. https://doi.org/10.15778/RESIF.RD

Ritter, J. R., Fröhlich, Y., Sanz Alonso, Y., & Grund, M. (2022). Short-scale laterally varying SK (K) S shear wave splitting at BFO, Germany—Implications for the determination of anisotropic structures. *Journal of Seismology*, *26*(6), 1137–1156. https://doi.org/10.1007/s10950-022-10112-w

Royden, L. H. (1993). The tectonic expression slab pull at continental convergent boundaries. *Tectonics*, *12*(2), 303–325. https://doi.org/10.1029/92TC02248

Rümpker, G., Kaviani, A., Link, F., Reiss, M. C., & Komeazi, A. (2023). Testing observables for teleseismic shear-wave splitting inversions: Ambiguities of intensities, parameters, and waveforms. *Annales Geophysicae*, *66*. https://doi.org/10.4401/ag-8870

Rümpker, G., & Ryberg, T. (2000). New "Fresnel-zone" estimates for shear-wave splitting observations from finite-difference modeling. *Geophysical Research Letters*, *27*(13), 2005–2008. https://doi.org/10.1029/2000GL011423

Rümpker, G., & Silver, P. G. (1998). Apparent shear-wave splitting parameters in the presence of vertically varying anisotropy. *Geophysical Journal International*, *135*(3), 790–800. https://doi.org/10.1046/j.1365-246X.1998.00660.x

Salimbeni, S., Pondrelli, S., & Margheriti, L. (2013). Hints on the deformation penetration induced by subductions and collision processes: Seismic anisotropy beneath the Adria region (Central Mediterranean). *Journal of Geophysical Research*, *118*(11), 5814–5826. https://doi.org/10.1002/2013JB010253

Salimbeni, S., Pondrelli, S., Margheriti, L., Park, J., & Levin, V. (2008). SKS splitting measurements beneath northern Apennines region: A case of oblique trench-retreat. *Tectonophysics*, *462*(1–4), 68–82. https://doi.org/10.1016/j.tecto.2007.11.075

Savage, M. K. (1999). Seismic anisotropy and mantle deformation: What have we learned from shear wave splitting? *Reviews of Geophysics*, *37*(1), 65–106. https://doi.org/10.1029/98RG02075

Schmid, S. M., Bernoulli, D., Fügenschuh, B., Matenco, L., Schefer, S., Schuster, R., et al. (2008). The Alpine-Carpathian-Dinaridic orogenic system: Correlation and evolution of tectonic units. *Swiss Journal of Geosciences*, *101*(1), 139–183. https://doi.org/10.1007/s00015-008-1247-3

Schmid, S. M., Fügenschuh, B., Kissling, E., & Schuster, R. (2004). Tectonic map and overall architecture of the Alpine orogen. *Eclogae Geologicae Helvetiae*, *97*(1), 93–117. https://doi.org/10.1007/s00015-004-1113-x

Silver, P. G. (1996). Seismic anisotropy beneath the continents: Probing the depths of geology. *Annual Review of Earth and Planetary Sciences*, *24*(1), 385–432. https://doi.org/10.1146/annurev.earth.24.1.385

Silver, P. G., & Chan, W. W. (1991). Shear wave splitting and subcontinental mantle deformation. *Journal of Geophysical Research*, *96*(B10), 16429–16454. https://doi.org/10.1029/91JB00899

Silver, P. G., & Savage, M. K. (1994). The interpretation of shear-wave splitting parameters in the presence of two anisotropic layers. *Geophysical Journal International*, *119*(3), 949–963. https://doi.org/10.1111/j.1365-246X.1994.tb04027.x

Slovenian Environment Agency. (1990). Seismic network of the republic of Slovenia [Dataset]. International Federation of Digital Seismograph Networks. https://doi.org/10.7914/SN/SL

Swiss Seismological Service (SED) At ETH Zurich. (1983). National seismic networks of Switzerland [Dataset]. ETH Zürich. https://doi.org/10.12686/sed/networks/ch

University of Genoa (1967). Regional seismic network of north western Italy [Dataset]. International Federation of Digital Seismograph Networks. https://doi.org/10.7914/SN/GU

University of Trieste. (1993). Friuli Venezia Giulia Accelerometric network [Dataset]. International Federation of Digital Seismograph Networks. https://doi.org/10.7914/SN/RF

University of Zagreb. (2001). Croatian seismograph network [Dataset]. International Federation of Digital Seismograph Networks. https://doi.org/10.7914/SN/CR

Ustaszewski, K., Schmid, S. M., Fügenschuh, B., Tischler, M., Kissling, E., & Spakman, W. (2008). A map-view restoration of the Alpine-Carpathian-Dinaridic system for the Early Miocene. *Swiss Journal of Geosciences*, *101*(S1), 273–294. https://doi.org/10.1007/s00015-008-1288-7

Vignaroli, G., Faccenna, C., Jolivet, L., Piromallo, C., & Rossetti, F. (2008). Subduction polarity reversal at the junction between the western Alps and the northern Apennines, Italy. *Tectonophysics*, *450*(1–4), 34–50. https://doi.org/10.1016/j.tecto.2007.12.012

Vinnik, L. P., Krishna, V. G., Kind, R., Bormann, P., & Stammler, K. (1994). Shear wave splitting in the records of the German regional seismic network. *Geophysical Research Letters*, *21*(6), 457–460. https://doi.org/10.1029/94gl00396

Walther, M., Plenefisch, T., & Rümpker, G. (2014). Automated analysis of SKS splitting to infer upper mantle anisotropy beneath Germany using more than 20 yr of GRSN and GRF data. *Geophysical Journal International*, *196*(2), 1207–1236. https://doi.org/10.1029/94GL00396

Wolf, J., Creasy, N., Pisconti, A., Long, M. L., & Thomas, C. (2019). An investigation of seismic anisotropy in the lowermost mantle beneath Iceland. *Geophysical Journal International*, *219*(1), S152–S166. https://doi.org/10.1093/gji/ggz312

Wolfe, C. J., & Silver, P. G. (1998). Seismic anisotropy of oceanic upper mantle: Shear wave splitting methodologies and observations. *Journal of Geophysical Research*, *103*(B1), 749–771. https://doi.org/10.1029/97JB02023

ZAMG - Zentralanstalt für Meterologie und Geodynamik. (1987). Austrian seismic network [Dataset]. International Federation of Digital Seismograph Networks. https://doi.org/10.7914/SN/OE

Zhao, L., Paul, A., Malusà, M. G., Xu, X., Zheng, T., Solarino, S., et al. (2016). Continuity of the Alpine slab unraveled by high-resolution P wave tomography. *Journal of Geophysical Research: Solid Earth*, *121*(12), 8720–8737. https://doi.org/10.1002/2016JB013310